Texas Instruments Innovation Challenge: Europe Analog Design Contest 2015 Project Report

Baby Night Watch

Team Leader	Sérgio Branco, asergio.branco@gmail.com
Team Members	André Ferreira, andrefilipegoncalvesferreira@gmail.com Duarte Fernandes, dduartefernandes@gmail.com Ruben Carvalho, rubentscarvalho@hotmail.com João Lage, jmcelage@gmail.com
Advising Professor	Jorge Cabral, jcabral@dei.uminho.pt
University	University of Minho, Portugal
Date:	31/07/2015

Qty	Ti Part Number & URL	Qty	Ti Part Number & URL
1	BEAGLEBK	1	TMP007
1	TPS63060	2	CC2530
	Z-STACK		

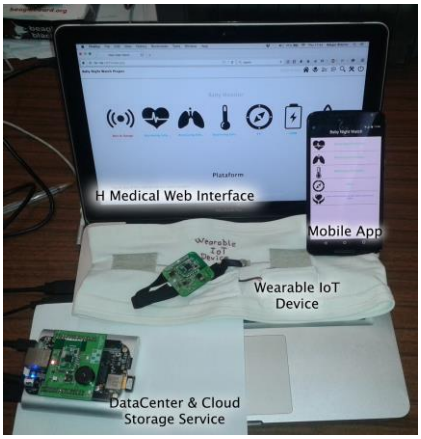

Project Abstract:

The Baby Night Watch aims to ensure infants' safety during sleep, by combining different emergent technologies (embedded systems, wearable devices, wireless communication, smart textiles, web-interfaces and mobile applications). The system is composed by the following elements: a Wearable IoT node, a Data Center and the H Medical Interface available for different platforms (smartphones, computers or tablets).The Wearable IoT Device is a wireless sensor node integrated in a Chest Belt with the capacity to monitor infants' physiological parameters, such as: body temperature, heart and respiratory rates, and capable of recognizing the sleeping position. After a minimal data processing, this set of information is sent continuously to the Data Center, which analyzes and stores the physiological infant's data, and makes it accessible to the user through the H Medical Interface. If a critical event occurs the device will trigger an alarm, visible and audible in the proximity, and sends a distress message to the mobile application. The H Medical Interface allows the users to visualize the collected information in real time. The Baby Night Watch can be used as an important tool for medical studies, since it allows access to previous physiological data and to export the database history to different types of datasets.
Through the experimental tests performed, the Baby Night Watch has proved to have the potential to identify situations that could potentially threaten an infant life.

1. Introduction and Motivation

Sudden Infant Death Syndrome (SIDS) is one of the major causes of death among infants, and it was the main motivator to design a wearable system capable to ensure the safety of a baby.

The project "Baby Night Watch" is a chest belt, so-called Wearable IoT Device with wireless communications capabilities capable of sensing signs that may lead to SIDS. A set of physiological parameters was selected as meaningful and descriptive of potential SIDS situations.

The infants' position during the sleep is one of this parameters for the evaluation of the quality of their sleep. Doctors say that the infants should sleep, preferential, on their back [1] and that they must not sleep on their belly, infants who sleep on their stomach are particularly vulnerable to SIDS due the increase risk of asphyxiation. Thus, we have developed an algorithm that allows the continuous monitoring of the infant' position during his sleep, based on the data retrieved from an accelerometer. The Baby Night Watch considers all the possible infant's positions: lying on his back, lying on his side (over the left arm and over right arm) and lying on his belly.

Two of the major signs that SIDS may be about to happen is abnormal breathing pattern and heart rate. Considering the following normal breathing rates: in the firsts six months of the newborn, the breathing rate is typically between 30 to 60 breaths per minute; 40 breaths per minute for an infant; after the first year it decreases, 24 to 30 breaths per minute [2]; to be able to detect breathing rate we used the same 3D digital accelerometer. Through the use of textile electrodes, integrated in the chest belt, the heart rate is measured by our system. The textiles revealed to be an excellent interface for bio-signal sensing, as they are flexible, stretchable and conform to the body (increasing the physical comfort of the infant), rendering them an interesting solution for ubiquitous, continuous health monitoring. A very small infrared temperature sensor checks the body temperature at regular intervals of time.

The main goal of the Baby Night Watch is to alert the parents, so the action time must be the minimal possible. The system can send alarms to the users by different ways, to ensure that help comes. Behind the metrics reliability and latency, the system has to operate continuously for long periods of time (over 8 hours), making the energy efficiency an important metric of the system. The main source of energy consumption is the wireless communications, corresponding to > 60% of the total of energy consumption in WSN or WBSN applications [3]. Therefore, to improve the battery's lifetime some features of the wireless transceiver were explored, as a way to develop an energy saving mechanism.

Although multiple technologies have been already created to prevent SIDS, they do not seem to be comfortable or they do not have the capacity to measure all the parameters. Also, alongside with the prevention, Baby Night Watch tries to be a continuous tool to study what may cause this Syndrome. Storing the information of any variation of patterns may be helpful to understand this syndrome.

1.1. Theoretical Background

Functional Requirements	• The Baby Night Watch is composed by a Wearable IoT Device, Data Center, H Medical Web Interface and Data Cloud Storage; • The Wearable IoT Device has to be capable of gather the following physiological and state parameters: breathing rate, heart rate, infant's position, body temperature and battery state; • Data Center has to recognize abnormal situations and send distress messages to the H Medical Web Interface; • H Medical Web Interface should allow the user to visualize the data in real-time, and should run in different platforms;
Non-Functional Requirements	• Wearable IoT Device is battery powered; • The heart rate has to be measured through a smart textile solution; • Wearable IoT Device is robust, biocompatibility, non-corrosive materials, non-intrusive, non-invasive; • Data Center is connected to the ZigBee coordinator node; • Data Center is powered and has Wi-Fi connection. • Each sensor have different sampling period; • Wearable IoT needs to support a dynamic output transmission power;

1.2. System Architecture

The Figure 1 illustrates the Baby Night Watch's architecture, where the different components and communication technologies used are depicted. The Wearable IoT Device collects different types of physiological data and sends the parameters to the Data Center (inside the belt's communication range). This off-body communication is made using the IEEE 802.15.4-compilant wireless transceiver radio, SoC CC2530, over the 2.4 GHz Industrial Scientific and Medical (ISM) band.

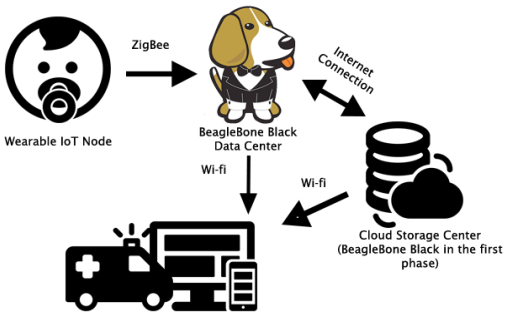

Figure 1. Baby Night Watch System's Architecture

The Data Center software analyses all the information sent by the Wearable IoT Device. If an unexpected event occurred, the Data Center will start buzzing and sending alarms to the Cloud Storage Center. The cloud stores the data and communicates with the H Medical Interface and the mobile applications connected to it[1]. The H Medical Interface allows users to check the baby's condition, retrieve previous stored data, visualize the collected information and export information in different types of files. To assure this interface is available in any device, the interface was totally implemented in web programming languages (Javascript, HTML5, CSS3, PHP and SQL). The CC2530 offers a wide range of output power transmission levels (from 4 dBm up to -22 dBm). This feature is explored on the energy saving mechanism developed to reduce the energy consumption in the wireless communication process. It consists on determination of the optimal transmission power output, i.e. the minimum output power to guarantee a successful delivery of packages.

2. System Design and Implementation

This section describes the different components of the Baby Night Watch project in terms of design and implementation strategy.

2.2. Wearable IoT Device

The Wearable IoT Device aquires the physiological parameters of the infant, parses it and sends processed data to the Data Center using the CC2530 SoC from Texas Instruments, through ZigBee wireless technology. The ZigBee stack selected for this project was the Z-Stack API. To reduce the size of the module we use the GB2530-L from GBAN (CC2530 with small form factor). A PCB with reduced dimensions (4.3x3.8x0.9cm) was designed to make it more comfortable. Since the device is battery powered, it uses a power supply system that includes the TI's TPS63060 to maximize the battery usage and its lifetime. The final PCB is shown in Figure 2. Since the battery voltage can be 3.7V (full battery charge) and the maximum voltage that can be read from an ADC pin on the CC2530 SoC is 3.3V (supplied voltage from the buck-boost), a resistor divider was used to measure the battery voltage (Figure 3). To minimize the power consumption of the Wearable IoT Device, a P-Mosfet was used to enable/disable this readout circuitry.

Figure 2. Wearable IoT Device: 3D Model representation, top and bottom view.

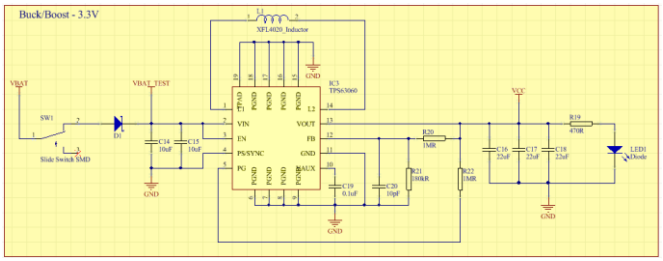

Figure 3. Buck/Boost converter schematic

2.2.1. *Heart Rate Sensor*

Since the goal of the system was not the acquisition of the full ECG[4], and considering the Wearable IoT requirements and constrains, a two-electrode sensor configuration was chosen [5]. The electrodes were knitted by the base-fabric, using a silver coated textured polyamide elastic yarn

[1] In this first phase the Data Center and the Cloud Storage Center are the same device

from Elitex, with low electrical resistance (in the order of tens of Ω/m). The wearable chest belt, composed by textile electrodes and conductive leads (to connect these elements to the analog front-end) were knitted by a MERZ MBS knitting machine depicted in Figure 4. For the electrode area, a particularly voluminous structure was developed, making the electrode area stand out of the rest of the fabric, and thus, improving the contact between skin and textile electrode. To ensure the correct positioning of sensors and signal acquisition hardware, the optimal electrode and sensor arrangements were studied. Regarding the electrodes for the heart rate acquisition, measurements with the electrodes at different positions in the chest area were carried out and compared. It was concluded that the best position is below the pectoral muscles, where the electrodes are closer to the ribs, avoiding electromyography interference.

Figure 4. MERZ MBS knitting machine.

To implement the heart rate measurement conditioning circuitry, an AD8232 was used and the heart rate monitor was designed to measure small biopotencial signals in noisy conditions, including analog low- and high-pass filters. The Instrumentation Amplifier has a gain of 100 V/V. The two-pole low-pass filter adds a gain of 11 V/V, resulting in an overall gain of 1100 V/V (Figure 5). Regarding the cutoff frequencies, the implemented block of the two-pole high-pass filter eliminates motion artifacts and drift caused by varying electrode-skin polarization and contact noise whilst the additional two-pole low-pass, using a Sallen-Key configuration, attenuates the line noise and other interference. Also, in this two-electrode configuration, the Right Led Drive (RLD) is used to drive the bias current resistors on the two electrode inputs, eliminating the third electrode needed. In addition, the AD8232 also offers two outputs called Leads Off Detection (LOD) + and -, one for each electrode, detecting when an electrode is disconnected by sourcing a small current (@100kHz) into them. When an electrode has lost its connection the corresponding LOD pin goes to a high-Z state. To compute the heart rate value, a CC2530 microcontroller was used in combination with the AD8232 as illustrated in Figure 6. Using its ultralow-power internal analog comparator, with a supply current of 230 nA, it is possible to compare the filtered ECG wave with an external voltage level. The analog comparator solution compares the voltage reference with the level of the ECG signal and the output changes when the ECG signal drops below the voltage divider value (voltage reference set to 300 mV). To calculate the infant's heart rate, a timer of the CC2530 is used to measure the time between two heart rate pulses. After fifteen triggers the average of these values is used to compute the heart rate.

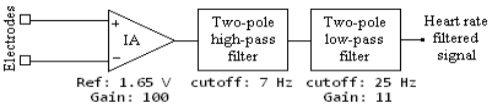

Figure 5. AD8232-EVALZ conditioning signal diagram.

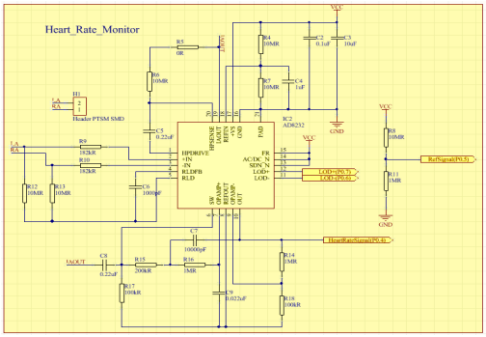

Figure 6 - Heart Rate Monitor schematics

2.2.2. *Infant's Position*

To detect the infants' position during the sleep the LSM330DLC inertial sensor from STMicroelectronics was used. In this project we did not use the built-in gyroscope. The LSM330DLC has 3 independent acceleration channels, a dynamically user-selectable full-scale range and, a SPI/I^{2}C serial interface. In Figure 7 the LSM330DLC schematic is depicted.

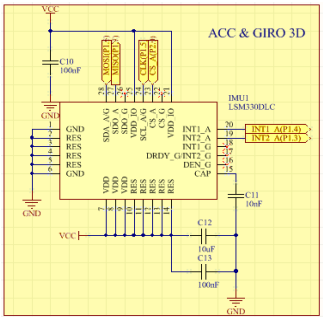

Figure 7. 3D Accelerometer schematics.

From Figure 8 the different positions of the infants are easily recognized by the force that the earth's gravity (±1g or ±9.81m/s^2) applies to each axis. Figure 8 also shows that the gravity force on the YY's axis is almost zero for all of the four possible positions and, therefore, YY is not used to determine the infant's position. When the infant is lying on his backs (scenario A), in

the ZZ's axis we will have ≈1g and on the XX's axis ≈0g. In scenarios B and D the infant is lying on his side, in the ZZ's axis we have ≈0g and in the XX's axis ≈-1g when the infant is lying over his left arm (scenario B) and ≈1g when the infant is lying over his right arm (scenario D). In scenario C the infant is lying on his belly and, in the ZZ's axis we have ≈-1g and in the XX's ≈0g. Also in Figure 8 the gray bars represent the transient stages between each position. Based on the information depicted in Figure 8, we have developed an algorithm for position recognition. To minimize the small fluctuations that can occur between accelerometer readings, a threshold value was defined that allows to control the tilt angle in which a position is defined. So, the working principle of the proposed algorithm is: if the accelerometer reading in one axis is higher than the threshold value and the reading of the other axis is lower than the defined threshold, the position is set according to the values read (i.e. if the value in the ZZ's axis is +1 g and the value in the XX's axis is 0, then the position of the infant is defined as lying on his back). To prevent unnecessary energy consumption, the position updates will only be send to the Data Center when a valid position change is detected.

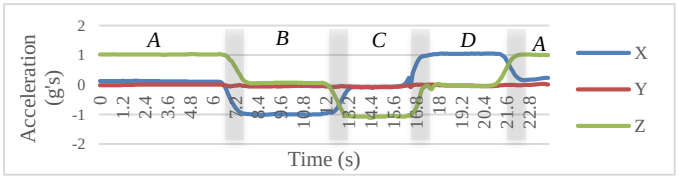

Figure 8 - Acceleration variation on each axis over positions changes

2.2.3. *Breathing Rate Sensor*

For measuring of the breathing rate, the same 3D accelerometer described above is used [6]–[9]. The sampling rate for the 3D accelerometer was set to 10 Hz, since it acquires the data at least ten times higher than the maximum frequency of the signal (60 breaths per minute). Figure 9 illustrates the data acquired in one of the accelerometer axis over a period of one minute. Due to the huge variations of the original signal between each sample (represented by the orange line), a smoothing algorithm based on the sliding window technique was employed, with a window of 10 samples or 1 second (blue line in figure above). As Figure 9 proves, the implementation of the smoothing algorithm results on a signal very similar to a breathing pattern and the data fluctuation is almost nonexistent.

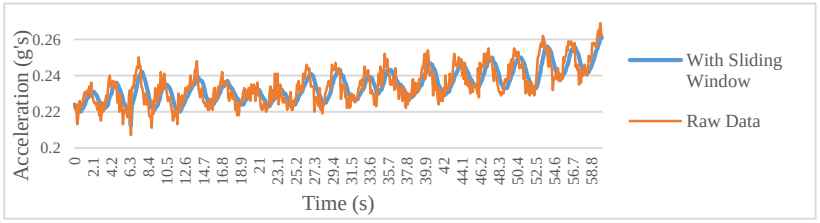

Figure 9. Smoothed and unsmoothed data acquired from the 3D accelerometer.

Since each breathing cycle has different amplitude and the techniques for peak detection require too much computational resources and, therefore have a huge energy consumption, a state machine with three possible states (Middle, High and Low) was used for obtaining the breathing rate, in order to minimize power consumption [7]. For the correct recognition and validation of a breathing cycle, the signal must follow this sequence: start on the Middle state; High state; Middle state; Low state and; Middle state again. The Middle state is defined by a threshold interval that sets the maximum and minimum breathing signal values. The selection of the threshold range is one of the key factors for the correct performance of the breathing rate sensor because, if this interval is too narrow the algorithm is likely to miss the transition between the Middle state, and if the interval is too large it is likely that the state machine never reach the Low or High state. Since the amplitude of the signal can be very small (0.219 g to 0.25 g, Figure 9), the selection of the threshold interval is very difficult due to the proximity of the values. So, the original signal was amplified on an order of a thousand times to make the selection of the threshold interval simpler. As it can be seen in Figure 9 the mean value of the breathing waveform can vary over the time. In order to prevent that this fluctuation might cause inaccuracies due to a static threshold interval, an average value of the signal over a limited period of

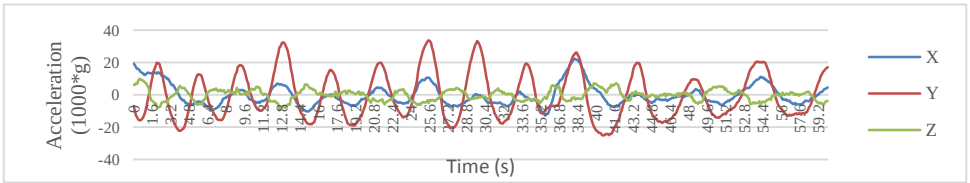

Figure 10. Axis's values while infant is lying on his back.

time was used, then this value was subtracted to the current smoothed value. With the implementation of this technique the system removes the continuous component of our signal and the resulting signal is the breathing pattern. Besides this, the system can use a static threshold interval, which means that it does not need to periodically compute the thresholds limits. This results in a reduction of the computation resources required and, consequently, on a more energy efficient algorithm. In Figure 10 and Figure 11 the resulting signal is depicted after the implementation of all the techniques described above, these techniques were applied for the three axis, during the same sampling period. Figure 10 and Figure 11 show the resulting signals over the three axis and during a period of 60 seconds, when the infant is lying on his back and when he is lying on his side, respectively. Through the analyses of both figures we can conclude, based on the signal amplitude, that the better representation of the breathing pattern is performed by the YY's axis and the ZZ's axis when the infant is lying on his back (Figure 10) and when he is lying on his side (Figure 11), respectively. If we give a closer look at Figure 11, it is possible to observe that although the ZZ's axis has a better breathing pattern (higher amplitude), some of the breathing cycles are below or slightly above of zero. This will means that the algorithm will be unable to recognize those cycles and this will lead to errors on the estimation of the number of breaths per minute. On the other hand, the breathing pattern of the YY's axis is more reliable because, although it has a lower amplitude, the breathing waveform is always around zero. So, with a careful selection of the threshold limits the algorithm is able to achieve a good performance.

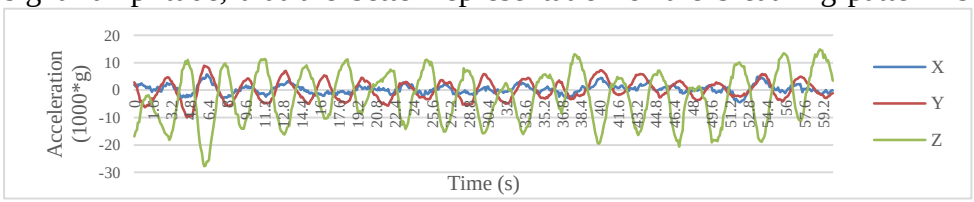

Figure 11. Axis's values while infant is lying on his side.

2.2.4. *Body Temperature*

For the measuring of the infant's body temperature an infrared thermopile sensor (TMP007) was used. The biggest advantage of the TMP007 is that it allows to measure the infant's body temperature without any contact with the skin of the infant. This makes our system less intrusive, more comfortable and, we have not to deal with problem of insufficient contact between the skin and the sensor. This sensor provides a digital interface (I^2C/SMBus) and his low power. The sensor circuitry is shown in Figure 12. The I^2C interface was used and so an API using the bit banging technique was developed and added to the Z-stack API. For a correct operation of the TMP007, namely the IR thermopile sensor, it must be thermally isolated from the PCB and other heat sources such as other components or, air currents. Figure 13 illustrates the PCB details for the thermal isolation of the TMP007 (placed on the bottom layer) from the rest of the PCB of the Wearable IoT Node.

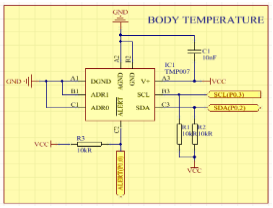

Figure 12. Body temperature schematics.

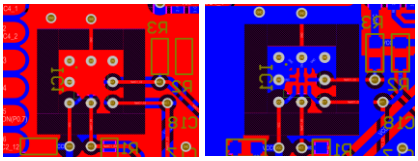
Figure 13. TMP007 PCB details, top and bottom layer.

2.3. Data Center

A BeagleBone Black, Debian Wheezy image installed, implements the Data Center. A lighttpd server with PHP 5.1 was installed on it to provide the network services. A shield, to the BeagleBone Black, with a buzzer, RGB led, push-button and a CC2530 was designed and implemented (Figure 14). The CC2530 communicates the information received by the Chest Belt using a Serial Port from the BeagleBone. The RGB led and the Buzzer are used to send distress messages every time a risk situation is detected. Different colors are used to tell the users which event occurred. The wireless USB adapter TL-WN725N is used to connect directly to the house's router. The BeagleBone stores the data received into the database. Unless some risk event occurs, the

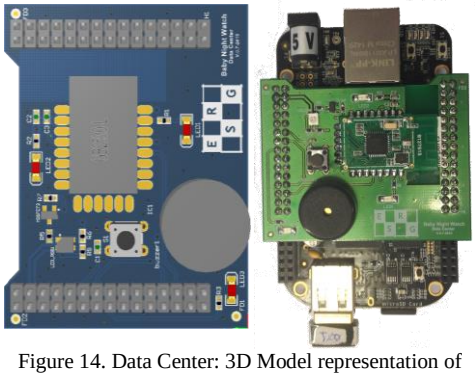
Figure 14. Data Center: 3D Model representation of the Data Center's Shield socket (Left); shield placement on the BeagleBone Black (right).

information received will only be store at regular intervals.

2.3.1. *H Medical Web Interface*

Figure 15 depicts the H Medical Web Interface, it was designed to help the user retrieve information from the Data Center. The web interface was developed in PHP, SQL, Javascript, HTML5 and CSS3. The main idea was to develop a full operational interface, which will work on any device, independently of the OS. To develop an interface that runs in a development board such as the BeagleBone Black, some of the processing power was switched to the user's side. To able to do that we used Javascript Programming Language. Besides Javascript taking off some processor work from BeagleBone it also turns the interface into a dynamic webpage, making it possible to monitor the baby in real-time. Some background PHP applications were created to fetch information to the web interface, to deal with the connection to the database. The H Medical Web Interface also allows the user to generate charts, time-lapse animations, and export data in different types of files. It's also prepared to receive new users, infants and to monitor them.

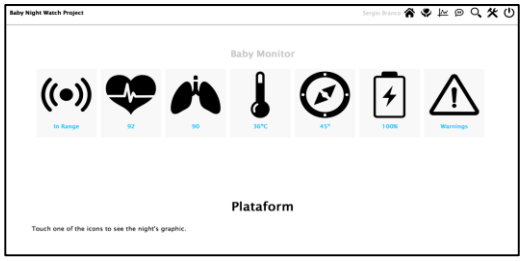

Figure 15. H Medical Web Interface.

2.4. Energy Saving based on TPC Mechanism

A TPC mechanism based on close-loop control was employed. It consists on a configuration of the current transmission output power at packet transmitter process (Wearable IoT node) based on the feedback information provided by the receiver (Data Center), as described in Figure 16. The Data Center is responsible for determining the Optimal minimum Output Power (OOP), i.e. the minimum output power to guarantee a successful delivery of packages. The new Output Power (OP) is determined based on the channel's state. The metric received signal strength indicator (RSSI) of the data frame sent by Wearable IoT device is used to predict the current channel's state. The information about the updated OP, so-called feedback information, is sent to the Wearable IoT device in form of a control frame. This device will upgrade the OP level, every time it receives a control frame. Those frames and future data frames are sent to the Data Center with the new OP.

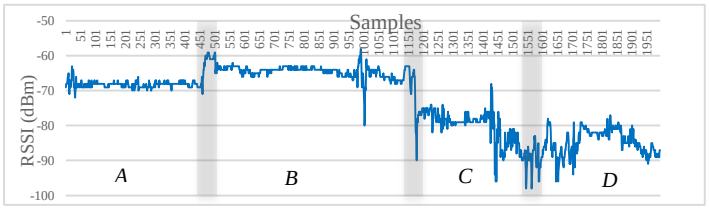

Figure 16. Received power signal for different baby positions and the transitions among positions (identified by a grey rectangle).

This process is repeated during the sensor nodes' lifecycle. Figure 17 illustrates the effect of each baby's position has in the channel behavior. At most favorable off-body communications scenarios (scenario A and B), the received signal is, essentially, due Line-of-Sight communication existence. The received signal revealed satisfactory values of RSSI and a behavior almost static, with short variations among samples, from 2 up to 4 dBm. The remaining scenarios, C and D, are the worst for wireless communications, as showed in Figure 16. It can be explained by the fact the final signal received is the combination of several multi-path components contribute, and also due the absence of the LOS component. Thus, the effect of the surrounding environment results in dynamic behavior of the received signal, i.e. extremely dynamic channel behavior in short periods of time (or among samples) and poor channel quality (RSSI values closer of the maximum receiver sensibility, -92 dBm in CC2530).

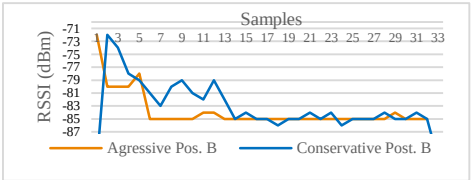

Figure 17. Channel Signals as result of application of Aggressive and Conservative TPL in a static environment (Position B).

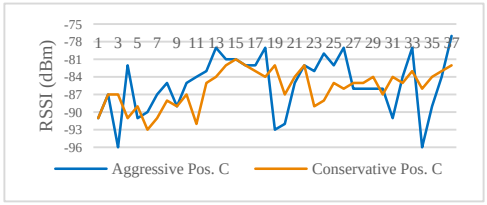

Figure 18. Wearable IoT signals as result of application of Aggressive and Conservative TPL in a dynamic environment (Position C).

The features of the electromagnetic waves, described above, suggest the inclusion of a target RSSI margin. In the case of the received signal RSSI be inside of the target margin, the OP will not be updated, otherwise a new value is determinate. The two distinct channel environments, small-signal and wide-signal variations environment, must be considered by the TPC mechanism simultaneously. For this reason, two techniques of output power determination are used in the Baby Night Watch system, a conservative and an aggressive TPC mechanism. Preliminary tests were performed, aiming to introduce a new vision about working principle, limitations of the two TPC techniques, and finally, a comparative analysis between them. During practical tests, the four user states/positions were considered. Tests were performed in an indoor environment (sleeping room4.0 x 3.0 m), while the Wearable IoT was located on the user chest and Data center located over the bedside table (distance among devices ≈ 3 m). The selected target RSSI margin range is from -87 dBm up to -80 dBm, and the sensor data from the Wearable IoT Device is collected every 3 seconds, during a period of 1.5 minutes to every user state. Figure 17 shows the signal's behavior over time, while the Baby Night Watch apply the aggressive TPL mechanism. Through comparison, it is possible verify that the aggressive mechanism is faster than the conservative, the latter requires more than 8 control frames to reach the optimal OP (-14 dBm), against the 2 frames of the aggressive mechanism. Figure 18 demonstrates that in a dynamic environment, like user position C and D, the signal does not stay within the RSSI margin target for long periods at the same OP (channel conditions vary rapidly). In this scenario the aggressive mechanism adjusts the OP exponentially farther from the target RSSI margin (switched 14 control frames), while the conservative adjusts the OP linearly around the target RSSI margin (switched 6 control frames). As a result, the aggressive TPL is the most suitable for static environment, while in dynamic environments, the conservative needs less control frames to reach the optimal OP and to keep within the target RSSI margin for more time.

```
Procedure aggressiveM ()
   nextOP= curRSSI;
   If curRSSI < thresholdMIN then
         nextOP←curOP + ((MaxOp−curOP)/2)
   else if curRSSI > thresholdMAX then
         nextOP←curOP/2;
   endif
   return nextOP;
End Procedure
Procedure conservativeM ()
   nextOP= curRSSI;
   If curRSSI < thresholdMIN then
         nextOP←curOP + 2;
   else if curRSSI > thresholdMAX then
         nextOP←curOP-2;
   endif
   return nextOP;
End Procedure
Procedure OPcontrol()
   If curScenario=='A' or curScenario=='B' then
         nextOP=aggressiveM();
   else if curScenario=='C' or curScenario=='D' then
         nextOP=conservativeM();
   endif
   If nextOP != curOP then
         return nextOP
   endif
End Procedure
```

Figure 19. Pseudocode of the TPC.

The proposed algorithm, pseudocode of the Figure 19, adjusts the OP based on the user position and on current state of the channel conditions. The conservative mechanism changes the OP linearly for dynamic environments. The aggressive mechanism changes the current OP exponentially; being suitable for dynamic scenarios, reducing the number of control frames sent to the Wearable IoT Device until it reaches the OOP.

3. Experimental Tests

In this section the experimental tests made, to evaluate each component of the Baby Night Watch system are described.

3.1. Heart Rate Sensor

The desired bio-signal was acquired for different infant's positions using NI-USB-6211 data acquisition device and NI Labview Signal Express software. The signals depicted in Figure 20 were obtained with the user standing still (scenario A). The waveforms represented in Figure 20 are the output of the Heart Rate monitor described before. Analog comparison with the 300 mV threshold used at the microcontroller's analog comparator delivers the heart rate pulses very robustly. As soon as movement is added, increasing motion artifacts will be present, as well as missed heart beat pulses due to momentary loss of contact of the electrodes with the skin. The signal in Figure 21 was acquired with vigorous movements. In this situation, some heart rate pulses are missing. These results were compared with commercial products (Polar model T-34 heart rate chest strap). From the experiments it was clear that the two systems behave similarly in terms of heart rate measurement, missing information under infant's

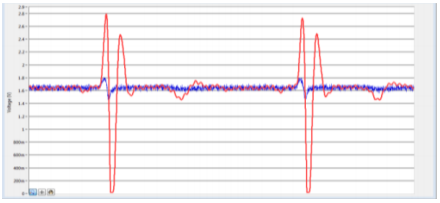

Figure 20. IA output (blue) and ECG filtered and amplified wave (red).

Figure 21. Arms moving vigorously while acquiring heart rate signal.

activity measurement conditions.

3.2. Breathing Rate Sensor

Experimental tests were conducted aiming to assess the proposed breathing rate sensor. These tests followed the same procedures as the ones carried out during the preliminary tests. Figure 22 shows the evaluation of the breathing waveform, across the three axis, during changes on the infant's position. As we can observe on the Figure 22, during position's changes (represented by the gray bar) the breathing pattern is disrupted but, the system was able to rapidly respond to that perturbation, it took ≈ 8 seconds. To prevent wrong estimations of the breathing rate, when the system detects a position's change it disable the breathing rate sensor until the new position is identified. During the tests the proposed algorithm for position detection was able to identify correctly the new position.

The overall performance of the breathing rate sensor was very good. When the infant was lying on his back (the recommend sleeping position), we achieved outstanding results (the algorithm was able to detect all the breaths). In this scenario the algorithm uses the data collected from the YY's axis. The data collected from the ZZ's axis are used to compute the BPM when the infant is lying on his side, as we got better results on this axis. In this scenario the results were not as good as the previous ones but the algorithm only misses one or two breaths on average, the worst case that we had was four breaths in one minute. A similar performance was achieved when the infant is lying on his belly but, in this situation, the data collected was from the YY's axis.

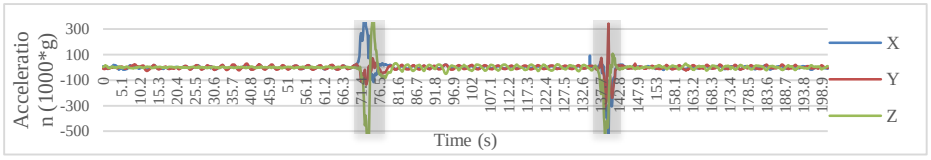

Figure 22. Breathing waveform during position's changes.

3.3. Transmission Power Control Mechanism

Experimental tests were conducted aiming evaluate the performance of the TPC algorithm suggested to the present application. The set of practical tests follow the same procedure of the preliminary tests, however, these tests took place in an environment with less reflectors objects (empty room, with a bed and bedtable). The evolution of TPC signal and signal emitted with a constant OP (4.5 dBm) is graphically represented in Figure 23 Through the figure is possible notice that the TPC algorithm revealed to be able to follow the dynamism of the channel communication environment, this is highlighted at the transition between positions (highlighted in the figure through the grey rectangles), where there is a fast-acting mechanism, ensuring that the signal remains within the margin even in the worst scenarios for communication, which were identified during the characterization phase of the channel (scenario C and D). The same TPC signal illustrated in Figure 23 is showed in Figure 25; additionally the OP used by the Wearable IoT during the transmission of the sensor data is showed in the same graph. It indicates that the system, in the present application, just need a few number of control packets to reach the OOP, and remaining within the target RSSI margin for a long periods of time, independently of the infant's position. The Figure 24 shows the energy consumption for the set of packets transmitted during the practical test, represented in Figure 25, and the total number of control packets emitted by the Data Center. The number of necessary control packets until reach the OOP is too low.

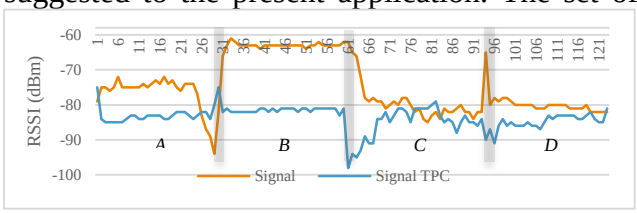

Figure 23. Channel's temporal behavior: packets sent at maximum OP and applying the TPC mechanism.

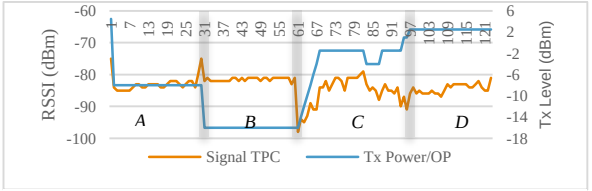

Figure 25. Channel's temporal behavior as result of the TPC mechanism and the updated OP by the TPC algorithm.

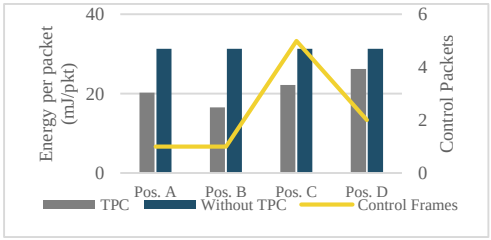

Figure 24. Energy Consumption per packet of TPC mechanism and total of control packet transmitted.

At the present test we checked that it is significantly lower than the number of packets used in the preliminary test, what the low number of reflector objects in the surrounding environment can justify. Therefore, we can state that a dynamic OP update allow us to reduce significantly the energy consumption (reduce ≈ 36 % of the total energy consumption during the wireless communication process to the user position A, ≈ 47 % position B, ≈ 30 % position C e ≈ 14 % position D), without affect the remaining requirements, namely reliable communication (a PER of 0% was verified) and low delay, furthermore the system reduce the amount of interference with coexist systems or devices.

4. Conclusions and Future Work

The Baby Night Watch is capable of detecting unexpected events and registering several physiological parameters, making it a powerful medical tool to understand SIDS, and a reliable real-time infant's monitor [10]. The project proved that with a small amount of hardware a huge number of parameters can be measured, improving the users experience and infant's safety. The lifecycle of the Wearable IoT Device (battery powered) was extended through an efficient TPC mechanism, turning it more compact and trustable. The data rate produced by the Wearable IoT Device is , in the order of 30 bytes per minute, easily supported by ZigBee, guaranteeing a desired small range of communication (meters), reducing the RF interference with other coexist devices and/or systems.

In the future some changes must be made to improve this project: placing the Cloud Storage Center into a webserver, allowing the users to retrieve information without having to be connected to the Data Center; implement some functionalities of the H Medical Web Interface in Python to improve stability and speed; use a more precise thermophile sensor to assure the body's temperature is more precise.

5. References

[1] Unknown, "Sleep Position: Why Back is Best." [Online]. Available: http://tinyurl.com/nuggzbf.

[2] H. Staff, "Normal Breathing Rates for Children." [Online]. Available: http://tinyurl.com/p8ba5eo.

[3] S. Movassaghi, M. Abolhasan, J. Lipman, D. Smith, and A. Jamalipour, "Wireless Body Area Networks: A Survey," *IEEE Commun. Surv. Tutorials*, vol. 16, no. 3, pp. 1658–1686, 2014.

[4] A. Catarino, H. Carvalho, M. J. Dias, T. Pereira, O. Postolache, and G. Pedro S., "Continuous health monitoring using E-textile integrated biosensors," *EPE 2012 - Proc. 2012 Int. Conf. Expo. Electr. Power Eng.*, no. Epe, pp. 605–609, 2012.

[5] D. E. J. Dias, M. F. Rocha, and A. Maria, "Tepzz 67_5z6a_t (11)," 2013.

[6] P. D. Hung, S. Bonnet, R. Guillemaud, E. Castelli, and P. T. N. Yen, "Estimation of respiratory waveform using an accelerometer," *2008 5th IEEE Int. Symp. Biomed. Imaging From Nano to Macro, Proceedings, ISBI*, pp. 1493–1496, 2008.

[7] a. Bates, M. J. Ling, J. Mann, and D. K. Arvind, "Respiratory rate and flow waveform estimation from tri-axial accelerometer data," *2010 Int. Conf. Body Sens. Networks, BSN 2010*, pp. 144–150, 2010.

[8] A. Jin, B. Yin, G. Morren, H. Duric, and R. M. Aarts, "Performance evaluation of a tri-axial accelerometry-based respiration monitoring for ambient assisted living," *Proc. 31st Annu. Int. Conf. IEEE Eng. Med. Biol. Soc. Eng. Futur. Biomed. EMBC 2009*, pp. 5677–5680, 2009.

[9] D. G. Pitts, M. K. Patel, P. Lang, a J. Sinclair, and R. Aspinall, "A respiratory monitoring device based on clavicular motion.," *Physiol. Meas.*, vol. 34, no. 8, pp. N51–61, 2013

[10] Team, "Demonstration Video." [Online]. Available: http://tinyurl.com/pb5fmtm.